Minimal Surfaces And Maximum Flows

Tabish Syed
tabish.syed@mail.mcgill.ca

August 2017

Contents

1 Introduction

Minimal surfaces are aesthetically beautifully, mathematically elegant and ubiquitous in nature. They are found in lipid membranes of cells and various other cell organelles[Terasaki et al., 2013] [Marshall, 2013], in the cuticle of insects [Galusha et al., 2008], wings of butterflies [Michielsen and Stavenga, 2008] [Saranathan et al., 2010], and various other organisms [Neville, 1993], and in structures like somatopod dactyl club [Weaver et al., 2012] in crustaceans. They are also found in the cochlea in the human ear and in the heart wall fibers

[Savadjiev et al., 2012]. Many materials with various desirable physical and electrical properties also have minimal surface structure [Torquato and Donev, 2004] [Thomas et al., 1988]. Interestingly, there is an analogous widespread presence of minimal surfaces in a variety of pure mathematical fields. Minimal surfaces arise in seemingly unconnected fields of topology, differential Geometry, calculus of variation, complex analysis, optimal transport and optimization.
The reasons of this extensive presence of such objects in various natural sturctures is however, not completely understood. Historically, the minimal surface problem was first described by Joseph-Louis Lagrange in 1762 in "Essai d'une nouvelle méthode pour déterminer les maxima et les minima des formules intégrales indéfinie", as a problem of variational calculus. Lagrange considered the problem of finding *a surface of minimal area stretched across a given closed contour.* However, it was Jean Baptiste Marie Meusnier in 1776 who gave two solutions, the catenoid (see figure 1a) and the helicoid (see figure 1b), to the problem. His solution also led to an alternate definition of the problem as *a surface with zero mean curvature everywhere.*

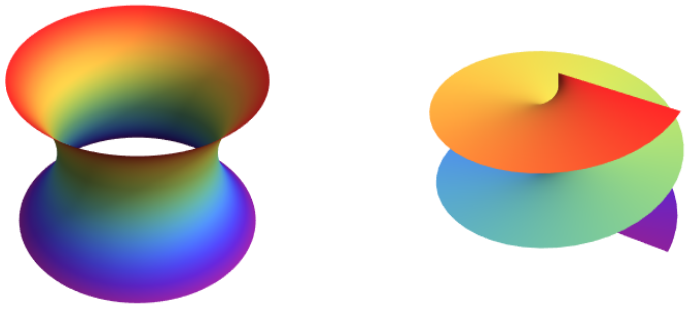

(a) Catenoid (b) Helicoid

Figure 1: First minimal surfaces to be discovered

In the following sections we discuss the equivalence of these two formulation, as well as other equivalent definitions. We note that these traditional minimal surfaces as well as their generalizations are extensively studied in Riemannian geometry and geometric measure theory. This extensive body of literature in these fields is beyond the scope of this report. We shall instead focus on a small subset of literature at the intersection of differential geometry and computer vision.
In computer vision, minimal surfaces arise in a variety of applications such as image segmentation [Caselles et al., 1997b], stereo matching [Buehler et al., 2002], shape matching [Windheuser et al., 2011] etc. In many such cases the problem is reduced to its discretized version of finding a *minimal-cut* in a graph. The problem of finding the minimal-cut is generally solved using *maximum flow* algorithms. Such a solution relies upon duality theorems of linear programs. We

give a brief review of the minimal-cut problem and its dual maximum flow in section 3. Further, in section 5, we provide details of how this standard problem in combinatorial optimization has been used in computer vision applications. We also review some works which extend the discrete problem into the continuous domain and the applications of this extension.
While the duality between the *minimal-cut* and the *maximum flow* problem has been extensive studied in the discrete domain, the equivalent duality in continuous domain between continuous flows and minimal surfaces has received scant attention. Specifically, the potential repercussions of such a duality for minimal surfaces found in nature has not been explored to the best of our knowledge.

2 Minimal Surfaces

2.1 Regular Surfaces

A surface u over a domain Ω is said to be *regular* at a point $\mathbf{x} \in \Omega$ if the tangent plane $T_{\mathbf{x}}u$ is well defined at $\mathbf{x}$. Further, the point $\mathbf{x}$ is said to be a *regular point* if u is regular at $\mathbf{x}$. For example, if u is a 2-dimensional surface then, at a regular point $\mathbf{x}$ the wedge product of the partial derivatives u_1, u_2, w.r.t x_1 and x_2 respectively, is non-zero. Equivalently, one may also define a *regular point* as a point on n dimensional surface where the Jacobian matrix has maximal rank n.
The unit *normal* $\mathbf{n}$ at a point p is defined as follows

$$\mathbf{n} = \frac{u_1 \wedge \cdots \wedge u_n}{|u_1 \wedge \cdots \wedge u_n|}$$

where u_i is the partial derivative of u w.r.t x_i at the point p. Note that the normal is well defined at all the *regular points*. We assume that all surfaces to be regular, except possible at isolated points.

2.2 Fundamental forms

Various metric properties such as length, area, curvature etc. of a surface may be calculated using *fundamental forms*.
The *first fundamental form* $I(\cdot, \cdot)$ over the tangent plane $T_{\mathbf{x}}u$ is equal to the inner product of the tangent vector. For $v, w \in T_{\mathbf{x}}u$ we have

$$I(v, w) := \langle v, w \rangle. \tag{1}$$

The coefficients of the *first fundamental form* are given by

$$g_{ij} := \langle u_i, u_j \rangle \tag{2}$$

where, u_i, u_j are the partial derivatives of u along i^{th} and j^{th} cordinates. The first fundamental form helps define a notion of length and area of a surface. Specifically, let u be a surface, whose *first fundamental form* is given by g_{ij}.

We define $W = |u_1 \wedge \cdots u_n|$. The *area element* of u is given by $dA = W\ dx_1 \wedge ... \wedge dx_n$.
The total area $A[u]$ of surface u is obtained by integrating dA over the entire domain Ω of the surface.

$$A[u] = \int_\Omega dA = \int_D W\ dx_1 \wedge ... \wedge dx_n \tag{3}$$

Note that we may equivalently write $W = \sqrt{g} = \sqrt{det(g_{ij})}$

The *second fundamental form* is a symmetric bi-linear form on the tangent plane, defined as follows

$$II(v, w) := \langle Sv, w \rangle \tag{4}$$

Where the *Weingarten map* $S : T_{\mathbf{x}}u \to T_{\mathbf{x}}u$ maps a vector $T_{\mathbf{x}}u \ni \mathbf{v} = v^i u_i$ (with implied summation over repeated index i according to the Einstein convention) as follow

$$v^i u_i \longmapsto -v^i \mathbf{n}_i$$

where, $u_i/\mathbf{n}_i$ is the partial derivative of $u/\mathbf{n}$ is the i^{th} coordinate direction. Note that the set $\{u_i\}$ forms a basis for the tangent plane $T_{\mathbf{x}}u$.
The coefficients of the *second fundamental form* are given by

$$b_{ij} := -\langle \mathbf{n}_i, u_j \rangle = \langle \mathbf{n}, u_{ij} \rangle \tag{5}$$

The second equality in (5) follows from the fact the $\langle \mathbf{n}, u_i \rangle = 0$, differentiation both sides we have $\langle \mathbf{n}_j, u_i \rangle + \langle \mathbf{n}, u_{ij} \rangle = 0$. The *second fundamental form* is useful in defining curvature of a surface.
Consider a surface $u(x, y)$. The eigenvalues of the *Weingarten map* S at a point p: κ_1, κ_2 are know as the *principal curvatures* of the surfaces at the point. The Gauss curvature K is defined to be $\kappa_1\kappa_2$, and mean curvature H is defined as $\kappa_1 + \kappa_2$ (we use sum instead of average of principal curvatures for ease of generalization to higher dimensions).
Let G, B be the first and second fundamental forms matrices of a surface and v be an eigen vector of S with eigen value κ. Then by definition of *second fundamental form* we have for any vector w

$$\begin{aligned}
\langle S(v), w \rangle &= v^T B w \quad \text{by definition} \\
\langle kv, w \rangle &= (B^T v)^T w \\
\kappa \langle v, w \rangle &= (Bv)^T w \quad \text{B is symmetric} \\
\kappa v^T G w &= (Bv)^T w \\
\kappa (G^T v)^T w &= (Bv)^T w \\
(\kappa G v)^T w &= (Bv)^T w \quad \text{G is symmetric}
\end{aligned}$$

We therefore have the eigen system

$$Bv = \kappa Gv$$

Therefore

$$H = \kappa_1 + \kappa_2 = Trace(G^{-1}B) = g^{ij}b_{ij}$$

and

$$K = \kappa_1\kappa_2 = det(G^{-1}B)$$

2.3 Minimal Surfaces

Let u_0 be a hyper-surface in $\mathbb{R}^{n+1}$ and $\mathbf{n}$ its unit normal. Given a vector field $V : u \to \mathbb{R}^{n+1}$ with compact support such that $V(\mathbf{x}) = 0 \; \forall \; \mathbf{x} \in \partial u$, where ∂u is the boundary of u. Let

$$u_s = \{x + sV(\mathbf{x}) : x \in u_0\}$$

where, s is a scalar parameter. The first variation of (nD) area is given by

$$\left.\frac{d}{dt}\right|_{s=0} Vol(u_s) = \int_{u_0} \mathrm{div}_{u_0} V \tag{6}$$

where, the divergence div_{u_0} is defined as follows

$$\mathrm{div}_{u_0} V = \sum_{i=1}^{n} \langle \nabla_{e_i} V, e_i \rangle \tag{7}$$

where, e_i is an orthonormal frame for u. The divergence of the component of V normal to u is given by

$$\begin{aligned} \mathrm{div}_{u_0} V^{\perp} &= \mathrm{div}_{u_0} \langle V, \mathbf{n} \rangle \mathbf{n} \\ &= \langle \nabla_{e_i} (\langle V, \mathbf{n} \rangle \mathbf{n}), e_i \rangle \\ &= \langle V, \mathbf{n} \rangle \langle \nabla_{e_i} \mathbf{n}, e_i \rangle \\ &= H \langle V, \mathbf{n} \rangle \end{aligned}$$

where H is the mean curvature scalar given by

$$H = \mathrm{div}_{u_0}(\mathbf{n}) = \sum_{i=1}^{n} \langle \nabla_{e_i} \mathbf{n}, e_i \rangle$$

Example 2.1 (Mean Curvature of a plane)**.** *Show that the mean curvature of the xy plane is 0.*

Proof. For the xy plane $\subset \mathbb{R}^3$, $\mathbf{n} = (0, 0, 1)$ at each point. Therefore

$$\nabla_x \mathbf{n} = \nabla_y \mathbf{n} = \nabla_z \mathbf{n} = 0$$

.

$$\Rightarrow H = \sum_{i=1}^{3} \langle \nabla_{e_i} \mathbf{n}, e_i \rangle = 0$$

■

From stokes theorem we have

$$\int_{u_0} \operatorname{div}_{u_0} V^T = 0$$

therefore,

$$\left. \frac{d}{dt} \right|_{s=0} Vol(u_s) = \int_{u_0} H \langle V, \mathbf{n} \rangle \tag{8}$$

From equation (8) we have the following definition for a minimal surface.

Definition 2.1. u is called a **minimal surface** if it has zero mean curvature everywhere.

If u is the graph of a function $u : \mathbb{R}^n \to \mathbb{R}$, then the upward-pointing normal is given by

$$\mathbf{n} = \frac{(-\nabla u, 1)}{\sqrt{1 + |\nabla_{\mathbb{R}^n} u|^2}}$$

and the mean curvature of u is given by

$$H = -\operatorname{div}_{\mathbb{R}^n} \left(\frac{\nabla_{\mathbb{R}^n} u}{\sqrt{1 + |\nabla_{\mathbb{R}^n} u|^2}} \right)$$

We then have the following alternative definition of a minimal surface

Definition 2.2. A surface u is a **minimal surface** if it satisfies the following differential equation.

$$-\operatorname{div}_{\mathbb{R}^n} \left(\frac{\nabla_{\mathbb{R}^n} u}{\sqrt{1 + |\nabla_{\mathbb{R}^n} u|^2}} \right) = 0 \tag{9}$$

Corollary 2.0.1. *For $u : \mathbb{R}^2 \to \mathbb{R}$ to be minimal , we have from* (9)

$$(1 + u_y^2) u_{xx} + (1 + u_x^2) u_{yy} - 2 u_x u_y u_{xy} = 0 \tag{10}$$

If we assume the surface to be constant upto first order, i.e u_x, $u_y \approx 0$, equation (10) approximates to $u_{xx} + u_{yy} = 0$ or $\Delta u = 0$, the Laplace equation. Therefore, the minimal surface equation may be interpreted as a non-linear generalization of the Laplace equation. We return to a discussion on the Laplace equation in section 2.4 to understand the relation between this "linear-approximation" and the original problem.

Example 2.2. *Show that a helicoid is a minimal surface*

Proof. A helicoid in $\mathbb{R}^3$ is given by $z = \arctan(\frac{y}{x})$, then

$$\begin{aligned}
\nabla z &= \left(\frac{-y}{x^2+y^2}, \frac{x}{x^2+y^2}\right) \\
\Rightarrow |\nabla z|^2 &= \frac{1}{x^2+y^2} = \frac{1}{r^2} \\
\Rightarrow H &= -\operatorname{div}\left(\frac{-y}{\sqrt{1+r^2}}, \frac{x}{\sqrt{1+r^2}}\right) \\
&= y \cdot \frac{1}{(1+r^2)^{\frac{3}{2}}} \cdot 2x \;-\; x \cdot \frac{1}{(1+r^2)^{\frac{3}{2}}} \cdot 2y \\
&= 0
\end{aligned}$$

■

Definition 2.3. From equation (6) we have, that u is **minimal** if and only if for all the vector fields V with compact support and vanishing on boundary of u

$$\int_u \operatorname{div}_u V = 0$$

2.4 Harmonic Functions

Let $u : \mathbb{R}^n \to \mathbb{R}$ be a differentiable function, then we define the *Dirichlet* integral as follows

$$E[u] = \frac{1}{2}\int |\nabla u|^2. \tag{11}$$

Let ϕ be an arbitrary smooth function with compact support and t be a parameter, then

$$\begin{aligned}
E[u + t\phi] &= \frac{1}{2}\int |\nabla(u + t\phi)|^2 \\
&= \frac{1}{2}\int |\nabla u|^2 + t\int \langle \nabla u, \nabla \phi\rangle + \frac{t^2}{2}\int |\nabla \phi|^2.
\end{aligned}$$

Differentiating w.r.t t at $t = 0$ we have

$$\begin{aligned}
\frac{d}{dt}\Big|_{t=0} E[u + t\phi] &= \int \langle \nabla u, \nabla \phi\rangle \\
&= -\int \phi \Delta u \quad \text{using green's identity}
\end{aligned}$$

From the above we may conclude that at critical point of *Dirichlet* integral we have

$$\Delta u = 0. \tag{12}$$

The solutions of equation (12) are known as *harmonic functions.*

Theorem 2.1. $A[u] \leq E[u]$

Proof. The result follows from the definition of $A[u]$ and $E[u]$ ■

Let u be a surface bounded by a curve Γ. Then if u minimizes $E[u]$ among harmonic surfaces, it can be shown that u minimizes $A[u]$. Unlike the area function $A[u]$, the energy $E[u]$ does not contain any square roots terms, and is therefore easier to work with. Further, equation (12) is a differential equation which may be solved numerically. The relation between energy and area, therefore, gives a practical method for working with minimal surfaces.
In addition to using the Laplace equation or the energy functional, the problem of finding a minimal surface may also be solved by either discretizing the problem and then reducing it to a discrete maximum flow problem, or transforming the problem into a continuous maximum flow problem and then solving the max-flow problem in continuous domain. Both these methods have been used in various applications in computer vision. In the following sections we introduce the minimal cut and maximum flow problems, discuss some applications of these problems in computer vision and indicate the relation to the minimal surface problem.

3 Minimal cut and Maximum Flow over Discrete Graphs.

3.1 Maximum Flow Over a Discrete Network

Consider a discrete graph $G(V, E)$, where V is the set of vertices and E the set of edges. Let $c_{ij} \in \mathbb{R}^+$ be the edge costs, interpreted as capacity, i.e, each edge (i, j) may support a flow $f_{ij} \leq c_{ij}$ (*Capacity Constraint*), where flow is a map $f : E \to \mathbb{R}^+$.
We require that the total flow into a vertex equals the total flow out. This constraint is violated at 2 special vertices s, t called the source (with excess out flow) and sink (with excess in flow) respectively. In other words, for each vertex $v \in V \setminus \{s, t\}$, net flow f_v vanishes:

$$f_v = \sum_j f_{jv} - \sum_i f_{vi} = 0 \qquad \textit{Conservation Constraint}$$

Consider a partition of the vertex set into collection $\Gamma_S = \{V_s, V_t\}$ such that $V_s \cap V_t = \phi$ and $V_s \cup V_t = V$ where $s \in V_s$ and $t \in V_t$. We associate a cost $C(\Gamma_S)$ to each partition Γ_S, equal to the sum of the costs of edges crossing from V_s to V_t:

$$C(\Gamma_S) = \sum_{i \in V_s} \sum_{j \in V_t} c_{ij}$$

The set of edges $(i, j) \in E$ such that $i \in V_s$ and $j \in V_t$, is called the *cut-set* E_x. The cost $C(\Gamma_S)$ may then be defined as the capacity of the *cut-set* E_x.

Definition 3.1. The *s-t minimal cut* problem seeks a partition which minimizes the cost such that nodes s (source) and t (sink) $\in V$ lie in disjoint sets.

Definition 3.2. The *maximum s-t flow* f in a graph $G(V, E)$ is the maximum amount of flow that may be routed from vertex s to vertex t, subject to the capacity and conservation constraints.

We now state a fundamental theorem regarding the minimal cuts and maximal flows in a graph, originally by [Ford and Fulkerson, 1956]

Theorem 3.1 (Min cut-Max Flow theorem)**.** *The maximal flow in the graph is equal to the minimal capacity cut. Furthermore, the maximum flow saturates the capacity of edges in the cut.*

$$\max f = \min C(\Gamma_S)$$

The original flow problem considered in [Ford and Fulkerson, 1956] is motivated by physical rail networks. However, there are a wide variety of problems which may be reduced to discrete network flow problem. In computer Vision, for example, the problem of image segmentation or stereo matching may reduced to a network flow problem over an appropriately defined graph. The continuous analogue of this problem, however, was studied in [Strang, 1983], [Iri, 1976] for the first time.

4 Minimal Surfaces and Continuous Maximum Flow

4.1 Maximum Flow Over Continuous Domains

The continuous extension of the max flow(P^*) - min cut(P) dual problems may be stated as follows.

$$\begin{aligned} (P^*) \quad \max \quad & \lambda, \\ \text{s.t} \quad & |\sigma|_* \leq c, \\ & \sigma \cdot n = \lambda f, \\ & \operatorname{div} \sigma = -\lambda F. \end{aligned}$$

$$\begin{aligned} (P) \quad \min \quad & \int\int |\nabla u| c \; dx \; dy \\ \text{s.t} \quad & \int\int uF \; dx \; dy + \int uf \; ds = 1. \end{aligned}$$

Where $F(x, y)$ gives the strength of sources distributed in the interior of domain Ω and $f(x, y)$ is the strength of sources along the boundary of the domain $\partial\Omega$

(assumed to be a simple closed Lipschitz curve).
We observe that the constraint $\operatorname{div}\sigma = -\lambda F(x,y)$ on smooth flow vector field $\sigma(x,y)$ is equivalent to the *Conservation Constraint* of the discrete setting. Note that for source free domains ($F(x,y) = 0$) , the *Conservation Constraint* reduces to $\operatorname{div}\sigma = 0$
The *Capacity Constraint* of the discrete setting manifests as a bound $|\sigma|_* \leq c(x,y)$ on the l^*-norm (dual to norm of ∇u in problem P) of σ in the continuous case. For feasibility we have [Strang, 1983]

$$\lambda = \int\int_{\Omega} \sigma \cdot \nabla u \; dx \; dy \leq \int\int_{\Omega} |\nabla u| c \; dx \; dy$$

Further for strong duality (equality) to hold, we require

$$\sigma = c\frac{\nabla u}{|\nabla u|} \quad \nabla u \neq 0$$

Then the min cut - max flow duality theorem for continuous case may be expressed as follows.

$$\max \lambda = \inf \int\int |\nabla u| c \; dx \; dy$$

4.2 Continuous Max flow For Minimal Surfaces

Motivated by the Push-relabel algorithm [Goldberg and Tarjan, 1986] for computing discrete maximum flow [Appleton and Talbot, 2006] proposed a method for computing continuous maximum flows by constraints relaxation.
Let σ be the flow in surface Ω containing source s and $\mathbf{n}$ be the normal to the surface Ω, such that $\operatorname{div}\sigma = 0$ (*Conservation Constraint*) and and $|\sigma| \leq c$ (*Capacity Constraint*). For σ_s, the net flow out of source s, we have

$$\sigma_s = \oint_{\Omega} \langle \sigma, \mathbf{n} \rangle d\Omega \leq \oint_{\Omega} c d\Omega$$

In order to solve for maximum flow, the authors relax the conservation constraint and consider the following system of partial differential equations

$$\begin{aligned} \frac{\partial V}{\partial t} &= -\operatorname{div}\sigma \\ \frac{\partial \sigma}{\partial t} &= -\nabla V \\ s.t \; |\sigma| &\leq c \end{aligned}$$

Where P is a scalar field such that at source s and at sink t: $V_s = 1$ and $V_t = -1$. This scalar field acts as a 'store' for the excess flow ($\operatorname{div}\sigma$). The minimal surface S_{min} is obtained from the zero level set of P.

4.3 Continuous Maximal Flows with anisotropic capacity constraints

[Zach et al., 2009] extend the isotropic flows considered in [Appleton and Talbot, 2006] to anisotropic capacity constraints.
Let $\phi : \mathbb{R}^n \to \mathbb{R}$ be a convex and positively 1-homogeneous (i.e $\phi(\lambda x) = \lambda\phi)(x)$) function. The *Wulff shape* W_ϕ is the set

$$W_\phi = \{y \in \mathbb{R}^n : \langle y, x\rangle \leq \phi(x) \ \forall \ x \in \mathbb{R}^n\}$$

Given a *Wulff shape* W_ϕ of function ϕ. The original function ϕ may be reconstructed by

$$\phi(x) = \max_{y \in W_\phi} \langle y, x\rangle = \max_{-y \in W_\phi} \langle -y, x\rangle$$

Consider a binary valued function $V : \Omega \to \{0, 1\}$. We define an energy function

$$E[V] = \int_\Omega \phi_{\mathbf{x}}(\nabla V) d\mathbf{x} \tag{13}$$

where $V(\mathbf{x}) = 1 \ \forall \ \mathbf{x} \in S$ and $V(\mathbf{x}) = 0 \ \forall \ \mathbf{x} \in T$. Since ϕ is convex and positively 1-homogeneous, we have $\phi(\nabla V) = \max_{y \in W_\phi} \langle -y, \nabla V\rangle$. Then,

$$E[V] = \int_\Omega \max_{-y \in W_\phi} \langle -y, \nabla V\rangle d\mathbf{x}$$

Let $\sigma : \Omega \to -W_\phi$ be a vector field, so that we may re-write the above equation and obtain the following optimization problem.

$$\min_V \max_\sigma E(V, \sigma) = \min_V \max_\sigma \int_\Omega \langle -\sigma, \nabla V\rangle \tag{14}$$

Differentiating we have

$$\begin{aligned} & \frac{\partial E}{\partial V} = \operatorname{div} \sigma \qquad \frac{\partial E}{\partial \sigma} = -\nabla V \\ s.t \quad & -\sigma(\mathbf{x}) \in W_{\phi_{\mathbf{x}}} \quad \forall x \in \Omega \\ & V(\mathbf{x}) = 1 \quad \forall \mathbf{x} \in S \\ & V(\mathbf{x}) = 0 \quad \forall \mathbf{x} \in T \end{aligned}$$

The gradient descent/ascent updates for the minimax optimization problem respectively are given by

$$\begin{aligned} \frac{\partial V}{\partial \tau} &= -\operatorname{div} \sigma \\ \frac{\partial \sigma}{\partial \tau} &= -\nabla V \end{aligned}$$

The gradient updates are then used to solve the optimization problem in equation (14) with generalized capacity constraints $\sigma(x) \in W_\phi \ \forall \ x \in \Omega$ on σ .

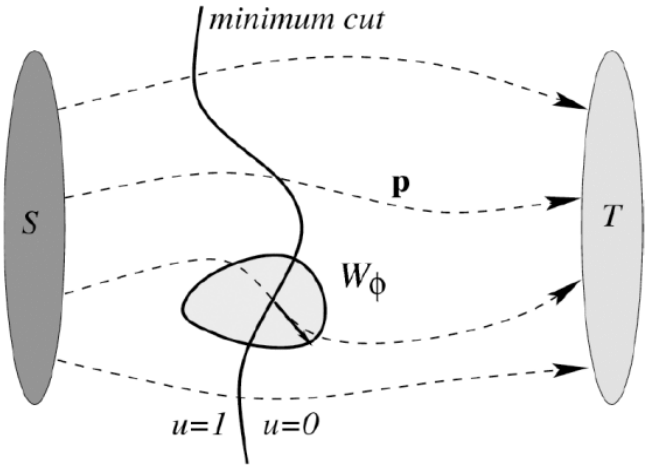

Figure 2: Continuous max flow with generalize constraints (Taken from [Zach et al., 2009])

Further [Zach et al., 2009] also obtain the dual energy to energy in equation (13) is given by

$$\begin{aligned} E^*(\sigma) &= \int_S \operatorname{div}\sigma \; dx \\ s.t \quad & \sigma \in -W_{\phi_{\mathbf{x}}} \\ & \operatorname{div}\sigma = 0 \quad \forall\, \mathbf{x} \in \Omega \setminus \{S, T\} \end{aligned}$$

Thus, the dual energy measures the net outflow from the source, which is a manifestation of the min-cut/max flow duality.

5 Applications of Minimal Surfaces

We now describe some applications, in computer vision, which use minimal surfaces theory to solve problems. A common thread among these applications is that they solve the minimal surface problem in a space where the metric is derived from the image content. While these applications do not provide any direct theoretical insights into the minimal surface problem, they do provide effective practical techniques for computing the solution of the problem.

5.1 Minimal Surfaces for segmentation

Geodesic active contours [Caselles et al., 1997a] is a classical object segmentation method which poses the object segmentation problem as one of finding a geodesic curve in a Riemannian space with metric derived from the image. The method uses curvature flows to evolve a deformable contour into an optimal boundary for image segmentation. In the 3D extension of the method

[Caselles et al., 1997c], [Caselles et al., 1997b] a deformable surface is used. The object boundary in this case is given by a *minimal surface* defined in a manner that is analogous to the 2D case. They pose the 3D image segmentation problem as one of minimizing a 'weighted' area, where 'weight' is derived from the image. Posing image segmentation as minimizing a weighted area essentially reduces the problem to the minimal surface problem. They show that the Euler Lagrange equation for the problem is

$$S_t = (gH - \nabla g \cdot \mathbf{n})\mathbf{n}$$

where g is the image dependent metric, H is the mean-curvature and $\mathbf{n}$ is the unit normal to 3D surface S_t. The solution of this Euler-Lagrange equation gives us a 3D minimal surface S, which forms the segmentation boundary. Using level set representation the evolution equations reduce to

$$\frac{\partial u}{\partial t} = g(I)|\nabla u| \left(\frac{\nabla u}{|\nabla u|} \right) + \nabla g(I).\nabla u.$$

The level set representation moves the (3D) problem to one higher (4D) dimension, and obtains a solution in the higher dimension. The solution of the original problem can then be computed from the zero level set of the higher dimensional problem. In the above equation, u is a 4D function with S as its 3D zero level set.

While the original motivation of this work is that of solving the image segmentation problem, the work gives a practical method for computing minimal surfaces directly (without using dual max-flow formulation).

5.2 Graph Cuts for Computing Minimal Surfaces

Section 5.1 describes the relation between optimal segmentation of an image and minimal surfaces with image derived metric. [Boykov and Kolmogorov, 2003] uses the well known graph cut segmentation technique [Boykov et al., 2001] to compute minimal Surfaces in 3D. They demonstrate the method by segmentating 3D structures in images. They use the Cauchy-Crofton formula, as described below, to estimate the length of a curve and minimize the length to obtain the final minimal surface.

The Cauchy-Crofton formula of integral geometry relates the Euclidean "length" of a curve to the measure of set of lines intersecting it. If $n_c(L)$ is the number of times any given line L intersects the curve C then the length $|C|_\epsilon$ of the curves is given by

$$|C|_\epsilon = \frac{1}{2} \int n_c d\mathcal{L}$$

where $d\mathcal{L}$ is the Lebesgue measure of the set of lines. Further, interpreting a cut C of a graph embedded in $\mathbb{R}^n$ as a closed surface, they define a *cut-metric* for graph given by

$$|C|_G = \sum_{e \in C} w_e$$

where C is a cut of the graph. Relating the length of curves to this cut metric, the problem of finding minimum cut is equivalent to finding "length/area" minimizing surface.
The authors use the this to pose image segmentation as a problem of finding an area mininimizing surface, where the "area" is derived based on image content.

6 Conclusion

In this report we gave a brief mathematical introduction to minimal surfaces and discussed their relation to maximum flows. We also discussed some application of minimal surfaces in computer vision.
We introduced, in section 2, the basic mathematical background for minimal surface. In sections 3, 4 we described the relation between the minimal surfaces, min cut problem and the max-flow problem and how the relations have been exploited in various applications (section 5). We pointed out in the introduction (Section 1) that physical minimal surfaces are ubiquitous in nature. While minimal surfaces have been studied extensively, the implications of dual maxumum flow for physical minimal surfaces has not been explored to the best of our knowledge. We plan on exploring the applications of the dual maximum flow in such physical minimal surfaces in future.

References

[Appleton and Talbot, 2006] Appleton, B. and Talbot, H. (2006). Globally minimal surfaces by continuous maximal flows. *IEEE Transactions on Pattern Analysis and Machine Intelligence*, 28(1):106–118.

[Boykov and Kolmogorov, 2003] Boykov, Y. and Kolmogorov, V. (2003). Computing geodesics and minimal surfaces via graph cuts. In *ICCV*, volume 3, pages 26–33.

[Boykov et al., 2001] Boykov, Y., Veksler, O., and Zabih, R. (2001). Fast approximate energy minimization via graph cuts. *IEEE Transactions on pattern analysis and machine intelligence*, 23(11):1222–1239.

[Buehler et al., 2002] Buehler, C., Gortler, S. J., Cohen, M. F., and McMillan, L. (2002). Minimal surfaces for stereo. In *European Conference on Computer Vision*, pages 885–899. Springer.

[Caselles et al., 1997a] Caselles, V., Kimmel, R., and Sapiro, G. (1997a). Geodesic active contours. *International journal of computer vision*, 22(1):61–79.

[Caselles et al., 1997b] Caselles, V., Kimmel, R., Sapiro, G., and Sbert, C. (1997b). Minimal surfaces: A geometric three dimensional segmentation approach. *Numerische Mathematik*, 77(4):423–451.

[Caselles et al., 1997c] Caselles, V., Kimmel, R., Sapiro, G., and Sbert, C. (1997c). Minimal surfaces based object segmentation. *IEEE Transactions on Pattern Analysis and Machine Intelligence*, 19(4):394–398.

[Ford and Fulkerson, 1956] Ford, L. R. and Fulkerson, D. R. (1956). Maximal flow through a network. *Canadian journal of Mathematics*, 8(3):399–404.

[Galusha et al., 2008] Galusha, J. W., Richey, L. R., and Bartl, M. H. (2008). High resolution three-dimensional reconstruction of photonic crystal structure found in beetle scales. In *IEEE/LEOS Summer Topical Meetings, 2008 Digest of the*, pages 83–84. IEEE.

[Goldberg and Tarjan, 1986] Goldberg, A. V. and Tarjan, R. E. (1986). A new approach to the maximum flow problem. In *Proceedings of the Eighteenth Annual ACM Symposium on Theory of Computing*, STOC '86, pages 136–146, New York, NY, USA. ACM.

[Iri, 1976] Iri, M. (1976). Theory of flows in continua as approximation to flows in networks. In *Survey of Mathematical Programming*, volume 2, pages 263–279.

[Marshall, 2013] Marshall, W. F. (2013). Differential geometry meets the cell. *Cell*, 154(2):265–266.

[Michielsen and Stavenga, 2008] Michielsen, K. and Stavenga, D. G. (2008). Gyroid cuticular structures in butterfly wing scales: biological photonic crystals. *Journal of The Royal Society Interface*, 5(18):85–94.

[Neville, 1993] Neville, A. C. (1993). *Biology of fibrous composites: development beyond the cell membrane*. Cambridge University Press.

[Saranathan et al., 2010] Saranathan, V., Osuji, C. O., Mochrie, S. G., Noh, H., Narayanan, S., Sandy, A., Dufresne, E. R., and Prum, R. O. (2010). Structure, function, and self-assembly of single network gyroid (i4132) photonic crystals in butterfly wing scales. *Proceedings of the National Academy of Sciences*, 107(26):11676–11681.

[Savadjiev et al., 2012] Savadjiev, P., Strijkers, G. J., Bakermans, A. J., Piuze, E., Zucker, S. W., and Siddiqi, K. (2012). Heart wall myofibers are arranged in minimal surfaces to optimize organ function. *Proceedings of the National Academy of Sciences*, 109(24):9248–9253.

[Strang, 1983] Strang, G. (1983). Maximal flow through a domain. *Mathematical Programming*, 26(2):123–143.

[Terasaki et al., 2013] Terasaki, M., Shemesh, T., Kasthuri, N., Klemm, R. W., Schalek, R., Hayworth, K. J., Hand, A. R., Yankova, M., Huber, G., Lichtman, J. W., et al. (2013). Stacked endoplasmic reticulum sheets are connected by helicoidal membrane motifs. *Cell*, 154(2):285–296.

[Thomas et al., 1988] Thomas, E. L., Anderson, D. M., Henkee, C. S., and Hoffman, D. (1988). Periodic area-minimizing surfaces in block copolymers. *Nature*, 334(6183):598–601.

[Torquato and Donev, 2004] Torquato, S. and Donev, A. (2004). Minimal surfaces and multifunctionality. In *Proceedings of the Royal Society of London A: Mathematical, Physical and Engineering Sciences*, volume 460, pages 1849–1856. The Royal Society.

[Weaver et al., 2012] Weaver, J. C., Milliron, G. W., Miserez, A., Evans-Lutterodt, K., Herrera, S., Gallana, I., Mershon, W. J., Swanson, B., Zavattieri, P., DiMasi, E., et al. (2012). The stomatopod dactyl club: a formidable damage-tolerant biological hammer. *Science*, 336(6086):1275–1280.

[Windheuser et al., 2011] Windheuser, T., Schlickewei, U., Schmidt, F. R., and Cremers, D. (2011). Geometrically consistent elastic matching of 3d shapes: A linear programming solution. In *Computer Vision (ICCV), 2011 IEEE International Conference on*, pages 2134–2141. IEEE.

[Zach et al., 2009] Zach, C., Niethammer, M., and Frahm, J.-M. (2009). Continuous maximal flows and wulff shapes: Application to MRFs. In *Computer Vision and Pattern Recognition, 2009. CVPR 2009. IEEE Conference on*, pages 1911–1918. IEEE.